*Desalination and Water Treatment*
www.deswater.com
doi: 10.5004/dwt.2019.24443

166 (2019) 321–333
October

# Adsorption mechanism of Cu(II) and Pb(II) from aqueous solutions using citric acid modified beet pulp fiber (CDSBP) and Fe-modified CDSBP

Ziyuan Gao, Qiang Liu, Huan Wang, Na Xia, Siming Zhu*

*School of Food Science and Engineering, South China University of Technology, Guangzhou 510641, China, Tel./Fax: +86 20 87113668; email: lfsmzhu@scut.edu.cn (S. Zhu), Tel. +86 13246838060; email: gzysoov@163.com (Z. Gao), Tel. +86 18718400356; email: 1039107750@qq.com (Q. Liu), Tel. +86 17875233010; email: 569417247@qq.com (H. Wang), Tel. +86 13379750976; email: 52460497@qq.com (N. Xia)*

Received 4 November 2018; Accepted 20 May 2019

**ABSTRACT**

A novel adsorbent (FCDSBP) from de-pectinated sugar beet pulp (DSBP) was successfully prepared by loading the surface of citric acid modified DSBP (CDSBP) with amorphous Fe-oxide species and FCDSBP was used to investigated the removal of metal ions ($Cu^{2+}$ and $Pb^{2+}$) from aqueous solutions. The obtained composites were characterized by FTIR, XRD and SEM. According to all characterization results, amorphous iron oxides of $FeO_x$ type and hydroxylated oxide were located on the FCDSBP surface. Due to the presence of amorphous Fe-oxide species and hydroxylated oxide, the adsorption capacity of FCDSBP for $Cu^{2+}$ and $Pb^{2+}$ was approximately three times that of CDSBP. In addition, the obtained experimental data of adsorption of metal ions by the FCDSBP and CDSBP fitted the Langmuir isotherm model well, and the pseudo-second-order kinetic model could be used to describe adsorption process. According to the calculated thermodynamic parameters, the metal ions adsorption process was endothermic and spontaneous in nature.

*Keywords:* Sugar beet pulp; Modification; Citric acid; Amorphous iron oxides; Adsorption mechanism; Heavy metal

## 1. Introduction

Heavy metals in water are potential threat to human health and have already caused undesirable effects on ecological environment. Contamination of water from heavy metal pollutants is a worldwide environmental problem due to their toxicity and non-biodegradable nature. The excessive indigestion of heavy metals contaminated water could cause symptoms such as cramps, vomiting or nerve functional disease [1,2]. Thus, efforts to efficiently and quickly remove heavy metals in water are crucial for human health and water purification.

To remove heavy metal ions from wastewater, numerous treatment processes, such as ion exchange [3,4], chemical precipitation [5], adsorption on activated carbon [6,7], membrane filtration [8] and coagulation [9], are currently used in practical applications. These methods have good scavenging effect, but also have high material costs and complicated operational processes. Therefore, most of them are not applicable in industry applications. In recent years, many researchers have focused on the removal of toxic heavy metal ions from aqueous solutions by using adsorption techniques with low-cost and environmentally friendly biomass materials. Numerous investigated biosorbent materials are obtained from waste biomass and available in different parts of the world, such as the wheat residue [10], dry tree leaves [11–13], rice hulls [14,15], mangosteen peel [16], tea waste [17], and marine alga [18]. However, most of the raw materials do not show satisfactory sorption capacity toward metal ions. Adsorption of heavy metal ions is due to

* Corresponding author.

physicochemical interaction, mainly the coordination effects between the metal ions and the functional groups, especially carboxylic acid groups (–COOH) [19]. That is to say, rational structure modification would enhance the adsorption performance of raw materials toward metal ions. For instance, tartaric acid treated rice husk has been reported to remove copper from aqueous solution [20]. Adsorption studies to determine the maximum adsorption capacity ($Q_{max}$) of modified rice husk toward copper was developed. Modified rice husk exhibited a maximum adsorption capacity of 29 mg $g^{-1}$ for $Cu^{2+}$ according to Langmuir model. Compared with unmodified rice husk, the adsorption capacity of tartaric acid modified rice husk has improved nearly six times. Furthermore, multiple studies have shown that chemical modification has a positive effect on the adsorption capacity of raw materials toward metal ions [21–23].

Sugar beet pulp (SBP), a by-product from beet sugar industry, is one of the largest agricultural residues in China. In fact, SBP comprises 20% cellulosic substances and more than 40% pectic substances [24]. The pectic substances are complex heteropolysaccharides, containing arabinose, galactose, and galacturonic acid. Pectic substances could bind metal cations in aqueous solution owing to the carboxyl functions of galacturonic acid [25]. In other words, SBP exhibits good potential as a metal adsorbent. Recently, several researchers have reported the application of SBP as metal scavengers for the removal of nickel [26], copper [27], and chromium [28].

Polymer metal complexes consist of a polymer ligand and metal ions. In the complexes, the metal ions are attached to the polymer ligand by a coordinate bond. The complexes show structural diversity, benefiting to better polymer physical and chemical behavior [29]. Polymer metal complexes are widely applied in many fields, especially in the catalyst research field [30]. The properties of polymer metal complexes depend on the nature of the metal ion and its content in the compounds. On the other hand, selecting appropriate ligands is crucial to determine the properties of the resulting complexes [31]. Furthermore, previous studies have shown that the adsorption capacity of raw materials pretreated with various iron compounds toward metal ions could be increased significantly [32–35]. For example, iron oxides can be used as active sorbents and play an important role in the adsorption of many ions.

Approximately 10 million tons of SBP is left after extracting sugar from sugar beet each year in China. Due to its rich polysaccharide content, SBP is used as a good source of pectin. De-pectinated SBP (DSBP) is an important biomaterial consisting of a small percentage of lignin, 20%–30% hemicelluloses and 40%–50% cellulose, it is considered as an ideal supporting material or carrier for the polymer metal complex in practical application. However, the solid residue of pectin-extracted SBP is usually burnt, causing potential environment pollution and a lot of waste of resources.

Thus, this study aimed to prepare heavy metal ions adsorbent using DSBP. DSBP may have high methoxyl pectin residues which gel at low pH values in aqueous solutions and have no application in the biosorption of metals, thus demethylation occurs at low temperatures and in an alkaline media [36]. The residue solid was modified with citric acid to introduce carboxylic groups through an industrialized pad–dry–cure process to obtain an esterified modified sugar beet pulp fiber (CDSBP). Subsequently, the obtained citric acid-esterification sugar beet pulp fiber (CDSBP) was coordinated with $Fe^{3+}$ ions to produce carboxylic fiber iron complex (CDSBP-Fe). Finally, the complex was hydrolyzed by mixing with alkaline media to form the iron modified sugar beet pulp fiber (FCDSBP) which is extremely stable and has a red brown color.

In our study, the performance and evaluation of two modified materials (CDSBP and FCDSBP) from de-pectinated pulp to adsorb heavy metal ions ($Cu^{2+}$ and $Pb^{2+}$) in aqueous solutions were described. In addition, the thermodynamics, equilibrium isotherms, and kinetics of batch adsorption were discussed. Finally, the characterizations of prepared composites were described to evaluate the synthetic effectiveness.

## 2. Materials and methods

### 2.1. Materials and chemicals

Sugar beet pulp was obtained from Lvxiang Sugar Company (Xinjiang, China). Prior to the experiments, impurities were removed from sugar beet pulp by washing with distilled water three times at room temperature. Cleaned sugar beet pulp was then dried in an oven at 50°C for 24 h to constant weight, grounded with a blender, and sieved to obtain particles with the diameter of 150–250 μm. The powder was stored for further experiments.

Citric acid (CA), hydrochloric acid (HCl, 37%), sodium hydrate (NaOH), ferric chloride ($FeCl_3{\cdot}6H_2O$), cupric sulfate ($CuSO_4{\cdot}5H_2O$), lead nitrate ($Pb(NO_3)_2$) were of analytical grade and used without further purification.

### 2.2. Preparation of the adsorbent

SBP fiber was prepared as following: the SBP powder was first treated with hydrochloric acid (85°C, pH 1.5 and 4 h) to remove pectin. The solid residue was washed with deionized water until no pH variation in wash water. The product was dried at 50°C until constant weight. The demethylation reaction occurred by mixing de-pectinated pulp (DSBP) with 0.5 M NaOH solution at a ratio of 1.0 g of material to 20 mL of solution. The mixture was shaken at 200 rpm for 1 h at room temperature. Subsequently, the material was placed on a gauze and washed with deionized water to remove excess base. The SBP fiber was dried in an oven at 50°C until constant weight and stored for further experiments.

The preparation of the adsorbent was in a consecutive two stage process as discussed in the upcoming sections.

#### 2.2.1. Stage (1): Modification of SBP fiber with citric acid

SBP fiber was mixed with various concentration citric acid at the ratio of 1:20 (fiber: acid, w/v) and stirred at 70°C for 60 min. The acid/fiber was dried at 50°C overnight. And the product was subsequently heated at 120°C for 120 min to obtain CA modified SBP fiber (denoted as CDSBP), which was washed thoroughly, rinsed, and dried.

Carboxyl group content in CDSBP sample ($Q_{COOH}$, mmol $g^{-1}$) was determined using a titration method [37].

Briefly, about 0.1 g of the dried CDSBP was treated with 100 mL of 0.01 mol $L^{-1}$ NaOH aqueous solution and stirred for 2 h at room temperature. The amount of the unneutralized NaOH in solution (25 mL) was titrated with an aqueous 0.01 mol $L^{-1}$ HCl solution. $Q_{COOH}$ values were calculated using Eq. (1).

$$C_{COOH} = \left[ \frac{\left(C_{NaOH} \times V_{NaOH}\right) - \left(4 \times C_{HCl} \times V_{HCl}\right)}{M_{mat}} \right] \quad (1)$$

where $C_{HCl}$ and $C_{NaOH}$ are the concentration of HCl and NaOH solution (mol $L^{-1}$), respectively. $V_{NaOH}$ is the volume of NaOH solution (100 mL), $V_{HCl}$ is the volume of HCl spent in the titration (mL), and $M_{mat}$ is the mass of CDSBP used (g).

#### 2.2.2. Stage (2): Coordination of CDSBP with $Fe^{3+}$ ions

1.0 g of CDSBP was mixed with 20 mL of the given concentration of $FeCl_3$ solution. The mixture was agitated for 3 h at 50ºC. The obtained CDSBP–Fe complex was then taken out, rinsed with distilled water to remove excess $FeCl_3$ solution. In order to calculate the Fe content ($Q_{Fe}$) of the complex, Varian Vista–MPX inductively coupled plasma optical emission spectroscopy (Optima 8300; PerkinElmer Co., USA) was used to determine the residual concentration of $Fe^{3+}$ ions in the coordinating solution. Subsequently, the complex was immersed in 0.1 mol $L^{-1}$ NaOH solution at a ratio of 1.0 g of material to 20 mL of solution. The mixture was shaken for 1 h at room temperature. The material was washed with deionized water to remove excess base and dried in an oven at 50°C until constant weight, which was designated as FCDSBP. The final product was stored for the following experiments.

### 2.3. Characterization of the adsorbent

The surface morphologies of original sugar beet pulp and modified sugar beet pulp were observed by scanning electron microscope (EVO 18; Carl Zeiss Inc., Germany) operating at 10 kV. The functional groups and chemical composition changes of sugar beet pulp fiber before and after modification were analyzed by Fourier transform infrared spectroscopy (Vector 33-MIR; Bruker Co., Germany) and X-ray diffraction (D/max-2200VPC; Bruker Co., Germany).

### 2.4. Batch adsorption experiments

The adsorbate solution was prepared by dissolving analytical grade cupric sulfate and lead nitrate in pure water to obtain the required concentration. Batch adsorption experiments involved equilibrating 0.5 g of CDSBP and 0.2 g of FCDSBP with 50 mL of aqueous solution at a given concentration in a beaker, respectively. The adsorption capacity of metal ions per gram of adsorbent was negligible after 30 min preliminary experiments. Therefore, a contact time of 30 min was used for batch tests. The effect of initial concentration of metal ions (400–1,300 mg $L^{-1}$), contact time (5–30 min), and pH (2–5) on single uptake was also studied. For pH values (2–5) adjustments, 0.1 mol $L^{-1}$ HCl and 0.1 mol $L^{-1}$ NaOH solutions were used.

### 2.5. Adsorption kinetics and isotherm experiments

To obtain the adsorption kinetic curves, adsorption experiments were carried out with a contact time ranging from 0 to 30 min. The mixture solution was shaken in a thermostatic shaker at a speed of 200 $min^{-1}$ and the solution was sampled at specific time intervals. For isotherm experiments, 50 mL of metal ion solution with six different initial concentrations ranging from 400 to 1,300 mg $L^{-1}$ were added into a conical flask, then a known weight of adsorbent was added. The adsorption was conducted at different temperatures for 30 min.

## 3. Results and discussion

### 3.1. Fabrication of adsorbent

SBP fiber was modified with citric acid to introduce the carboxyl groups, which coordinated with $Fe^{3+}$ ions for obtaining CDSBP–Fe complex, and the results are shown in Fig. 1.

Fig. 1a shows the effect of citric acid concentration on $Q_{COOH}$ values of the modified SBP fiber. Increasing initial citric acid concentration caused a gradual increment in $Q_{COOH}$ values of CDSBP, and proposing the maximum $Q_{COOH}$ values were achieved at citric acid concentration of 2 mol $L^{-1}$. This is because higher concentration of citric acid could enhance the esterification between carboxyl groups of citric acid and hydroxyl groups in cellulose surface on SBP fiber [38].

Fig. 1b displays a different change in $Q_{Fe}$ values of the obtained complexes prepared by CDSBP with varied $Q_{COOH}$ values. $Q_{Fe}$ values of the complex increased with their $Q_{COOH}$ values, and the highest $Q_{Fe}$ value was achieved at 2.1 mmol $g^{-1}$ of $Q_{COOH}$ value. This may be attributed to complex's complicated crosslink structure between cellulose chains. The crosslink structure may result in space steric hindrance and limit the coordination of $Fe^{3+}$ ions with their carboxyl groups. As shown in Fig. 1c, when CDSBP with $Q_{COOH}$ value (approximately 1.8 mmol $g^{-1}$) was used, $Q_{Fe}$ value of the resulting complex increased with the increasing initial concentration of $Fe^{3+}$ ions and reached a maximum value at 0.1 mol $L^{-1}$ of $Fe^{3+}$ ions.

Based on the above analysis, the preparation or modification process of CDSBP and FCDSBP is presented in Fig. 2.

### 3.2. Surface morphology and composition analysis

Fig. 3 presents the SEM micrographs of the dry original SBP taken before and after each treatment. It was observed that the surface morphological characters of untreated and treated SBP samples were quite different. As can be seen from Fig. 3a, the surface of the dry original SBP was rough. Fig. 3b shows that after the treatment with citric acid, the surface of the CDSBP became smooth and many small wrinkles were found. In Fig. 3c, after the coordination of CDSBP with $Fe^{3+}$ ions, a mud-like layer was found on some of wrinkles. The reason for the layer of rough or uneven surface may ascribe to the formation of CDSBP–Fe complex. The variation of morphological characters indicated that carboxyl groups of citric acid has been imparted to the surface of SBP fiber and resulted in coordination of CDSBP with $Fe^{3+}$ ions [39]. When Figs. 3c and d are compared, it

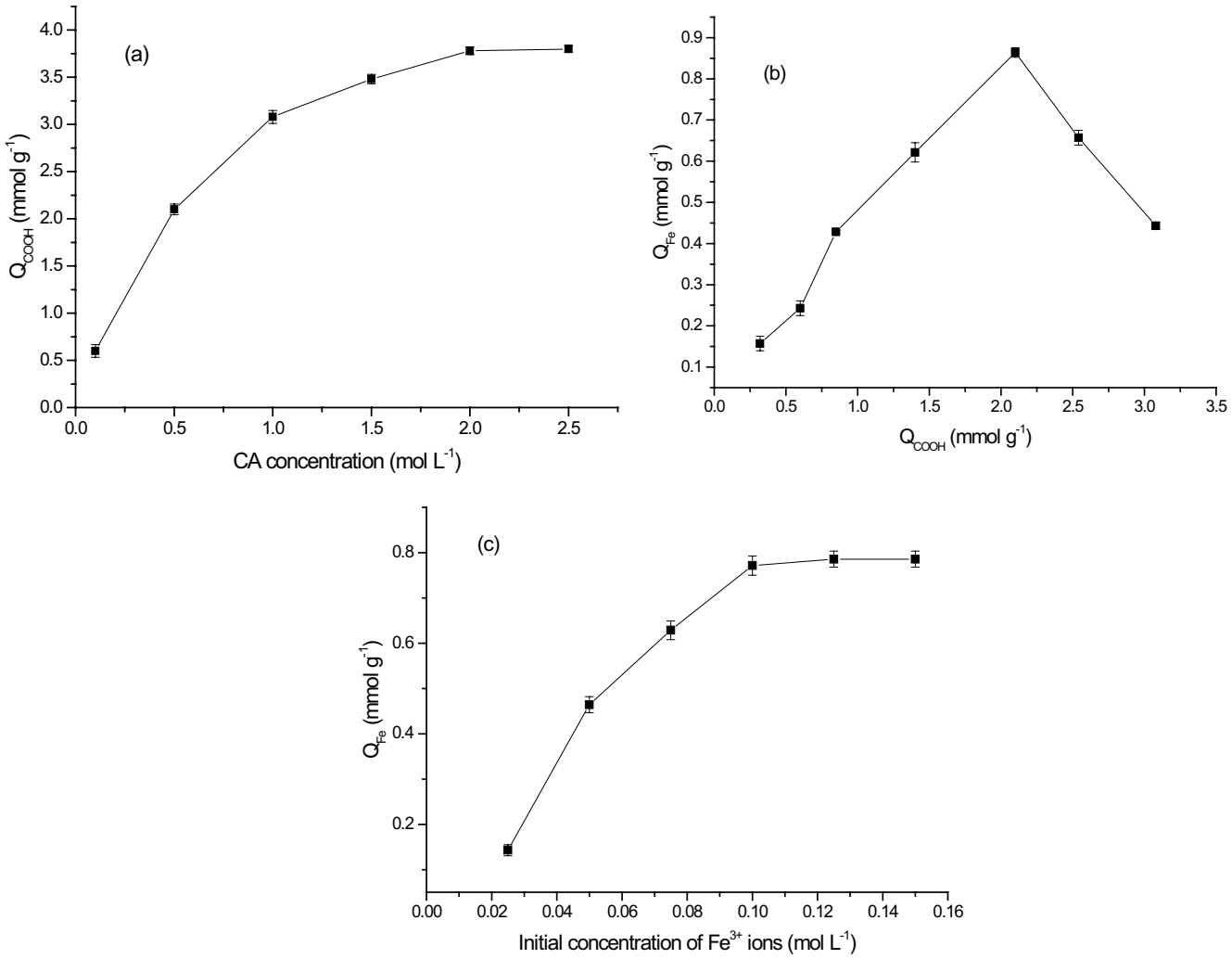


Fig. 1. Fabrication of CDSBP–Fe complex at different experimental conditions.

can be observed that the surface of FCDSBP became much smoother and had less small wrinkles, suggesting $Fe^{3+}$ ions reacted to bases and formed various Fe species.

Fig. 4a shows the FTIR analysis results, and major characteristic absorption peaks of original sugar beet pulp at 3,340; 2,900; 1,630 and 1,030 cm$^{-1}$ are owing to the stretching of O–H, C–H, COO–, and C–O–C, respectively. The bending vibration of C–H gets reflected in two peaks at 1,310 and 1,440 cm$^{-1}$ due to asymmetric and symmetric bending vibrations. The peak at 1,058 cm$^{-1}$ appearing in spectra is assigned to C–O stretching vibration, reflecting the characteristic of the cellulose structure [40]. Compared with the original sugar beet pulp, the peaks centered at 3,340; 2,900; 1,440; 1,310; and 1,030 cm$^{-1}$ became much less intensive in the spectrum of de-pectinated pulp, indicating that sugar beet pectin has been removed from the untreated SBP. A new peak around 1,740 cm$^{-1}$ were found in the spectrum of the of CDSBP, which could be attributed to the stretching vibration of the carboxyl groups and ester carbonyl bands of citric acid with sugar beet pulp, confirming that the carboxyl groups have been introduced into surface structure of sugar beet pulp by ester linkage with citric acid. More importantly, the intensity of bending mode at 1,740 and 1,630 cm$^{-1}$ became more intensive in the spectra of CDSBP–Fe complex. This result suggested that $Fe^{3+}$ ions coordinated with the carboxyl groups of CDSBP [39]. In the spectrum of FCDSBP, the band at 3,630 cm$^{-1}$ correspond to the free –OH disappeared, which indicated that this specific hydroxyl would not vibrate anymore due to the changes caused at active sites during the formation of the FCDSBP. The peak around 890 cm$^{-1}$ was assigned to Fe–OH stretching vibrations and a broad band at 3,730 cm$^{-1}$ indicated the increase in hydrogen bonding for FCDSBP.

The XRD patterns of sugar beet pulp before and after modification are shown in Fig. 4b. As can be seen from this figure, there was a sharp diffraction peak at 21.8° which is characteristic of typical cellulose I structure in all the samples XRD patterns [41]. This peak in the case of citric acid modified SBP fiber was much sharper and narrower than that of unmodified SBP fiber, indicating that citric acid treated samples have higher degree of crystallinity. The reason is that the citric acid molecule can penetrate the amorphous regions in SBP fiber more easily when SBP fiber was modified with citric acid. Then esterification process could produce crosslinks

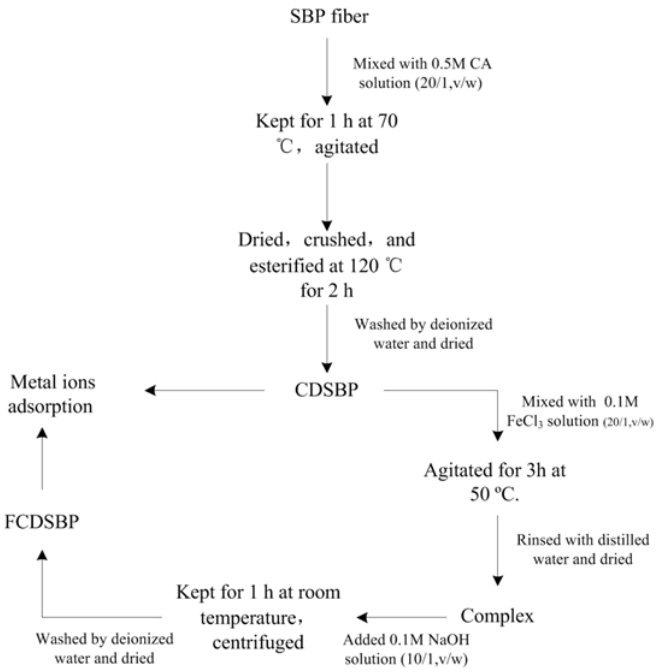


Fig. 2. Schematic diagram of the production process of CDSBP and FCDSBP.

between cellulose units in the amorphous regions, resulting in the increase of crystallinity [42]. Another obvious shoulder peak at 15.9° observed after citric acid modification can be attributed to the enriched structure of cellulose. The enrichment in cellulose may be due to the removal of amorphous fraction from the de-pectinated pulp. Although $Fe^{3+}$ ions may enhance the linkage between the cellulose units in the amorphous regions due to the coordination of $Fe^{3+}$ ions with carboxyl groups of CDSBP [43], the intensity of the sharp diffraction peak at 21.8° was reduced by subsequent coordination of CDSBP with $Fe^{3+}$ ions. It was possible that the strong acidity of $Fe^{3+}$ ions aqueous solution could cause a serious erosion of the crystal surface, reducing the crystal volume and leading to a decrease in crystallinity [44]. FCDSBP was characterized by lower crystallinity than the CDSBP–Fe complex. However, FCDSBP maintained the main characteristic peaks of cellulose with significantly lower intensity and had no other characteristic peaks in the diffraction peaks, indicating no additional Fe oxides or oxo-hydroxidic crystalline phases. Therefore, it could be predicted that no crystalline Fe-phases have been formed at FCDSBP surface sites.

### 3.3. Effect of the initial solution pH on adsorption equilibrium

As reported by numerous studies, pH plays an important role in the sorption uptake of metals on biomasses [45,46].

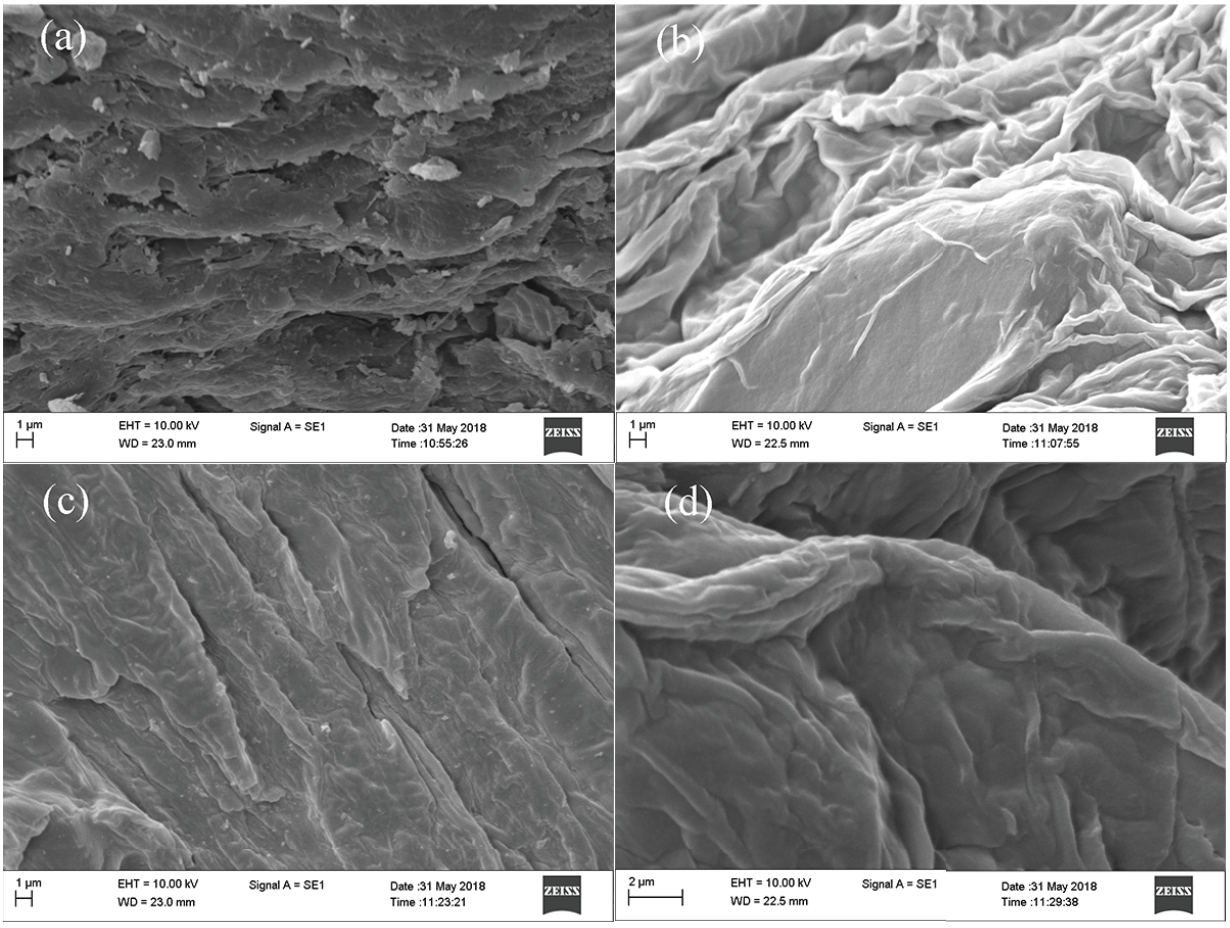


Fig. 3. SEM images of (a) SBP fiber, (b) CDSBP, (c) CDSBP–Fe complex, and (d) FCDSBP.

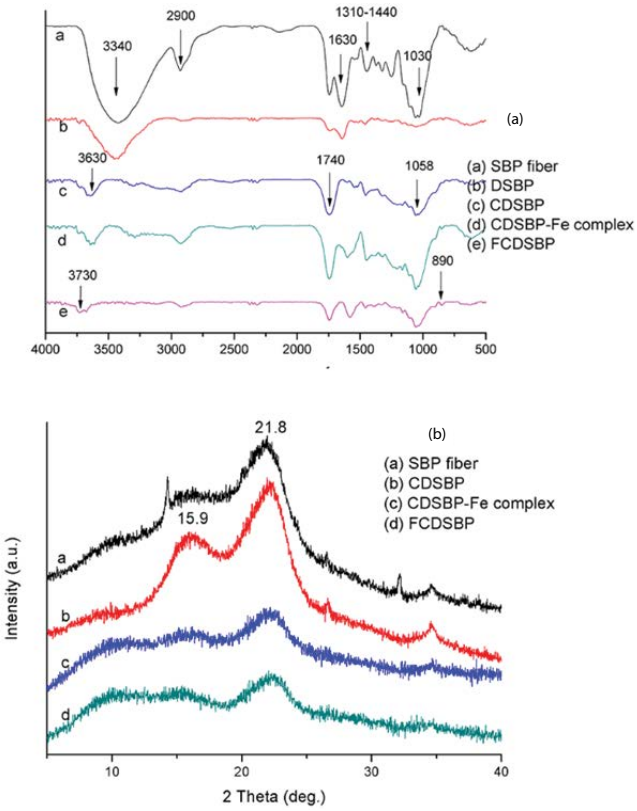


Fig. 4. (a) FTIR spectra and (b) X-ray diffraction patterns of original sugar beet pulp and modified sugar beet pulp fiber.

Fig. 5 shows the adsorption capacity of $Ca^{2+}$ or $Pb^{2+}$ per gram of adsorbent within the pH value range of 2–4.5. As shown in Fig. 5, the adsorption capacity of $Cu^{2+}$ or $Pb^{2+}$ was the minimum at pH = 2, and then it increased with increasing pH and reached up to a maximum value at pH 4.5. This phenomenon may be explained by the variation in interchangeable ions binding with the functional groups of the adsorbent matrix, such as $H^+$ ions. At low pH values, the concentration of $H^+$ ions was high in the solution, the functional groups on the surface of the adsorbent were easier to take positive charge, which would cause prominent electrostatic force of repulsion between adsorbent and the positively charged metal ions [47]. In addition, $H^+$ ions competed with $Cu^{2+}$ or $Pb^{2+}$ in the solution for the active sites. Therefore, the adsorbent exhibited a low adsorption capacity. Owing to high negative charge on the adsorbent surface at elevated pH values, the electrostatic attraction force between adsorbent and metal ions was prominent. Moreover, as pH increases, the competition between positively charged $H^+$ and $Cu^{2+}$ or $Pb^{2+}$ was weakened, resulting in a favored adsorption process [48]. At pH values greater than 5, the formed metal complex played a leading role during $Cu^{2+}$ and $Pb^{2+}$ removal process [49]. Hence adsorption of metal ions ($Cu^{2+}$ and $Pb^{2+}$) onto CDSBP and FCDSBP was at optimum pH of 4.5.

### 3.4. Adsorption isotherms

The equilibrium adsorption isotherm played a significant role in the adsorption mechanism. The adsorption isotherms of metal ions ($Cu^{2+}$ and $Pb^{2+}$) on CDSBP and FCDSBP at three different temperatures (298, 308 and 318 K) were analyzed. Experimental data were fitted to the Langmuir (Eq. (2)) and Freundlich (Eq. (3)) models and used to describe adsorption equilibrium.

$$q_e = \frac{q_m k_L C_e}{\left(1 + k_L C_e\right)} \tag{2}$$

$$q_e = K_F C_e^{1/n} \tag{3}$$

where $q_m$ is the maximum sorption capacity, $K_L$ is the Langmuir constant, and $K_F$ and $n$ are the Freundlich constants.

Fig. 6 shows the effect of initial metal ion concentration on adsorption capacity at different temperatures. Because the adsorption sites of CDSBP and FCDSBP were not fully used, the adsorption capacity per gram of CDSBP and FCDSBP for metal ions was low with lower initial concentration. The adsorption capacities of adsorbent on $Ca^{2+}$ and $Pb^{2+}$ reached a maximum value at a concentration of 1,000 mg $L^{-1}$ for $Ca^{2+}$

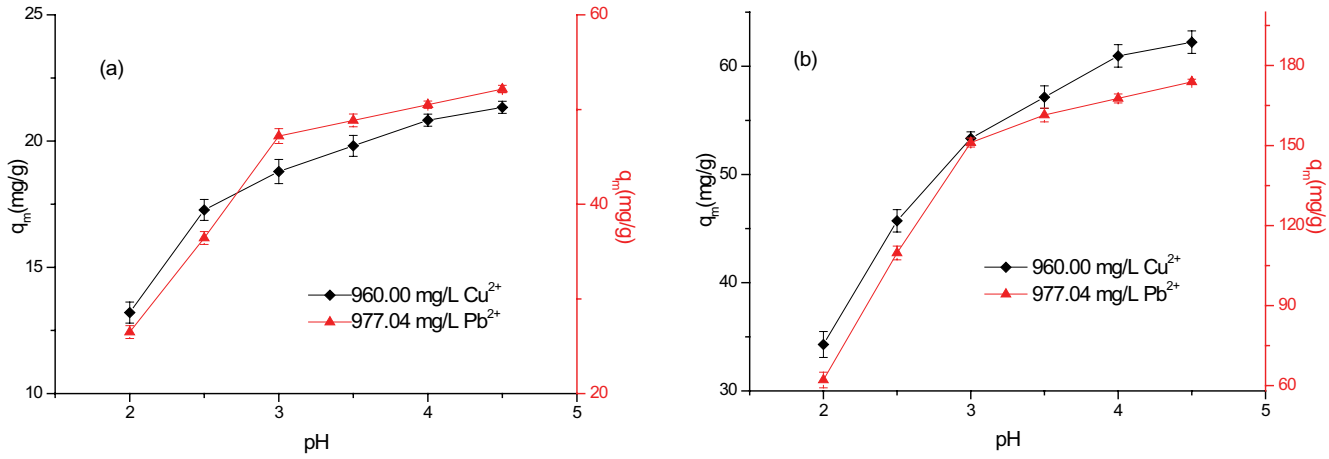


Fig. 5. Effect of pH on the adsorption of metal ions by (a) CDSBP and (b) FCDSBP: 0.5 CDSBP or 0.2 g of FCDSBP mixed with 50 mL $Ca^{2+}$ or $Pb^{2+}$ solution, respectively, at 30°C.

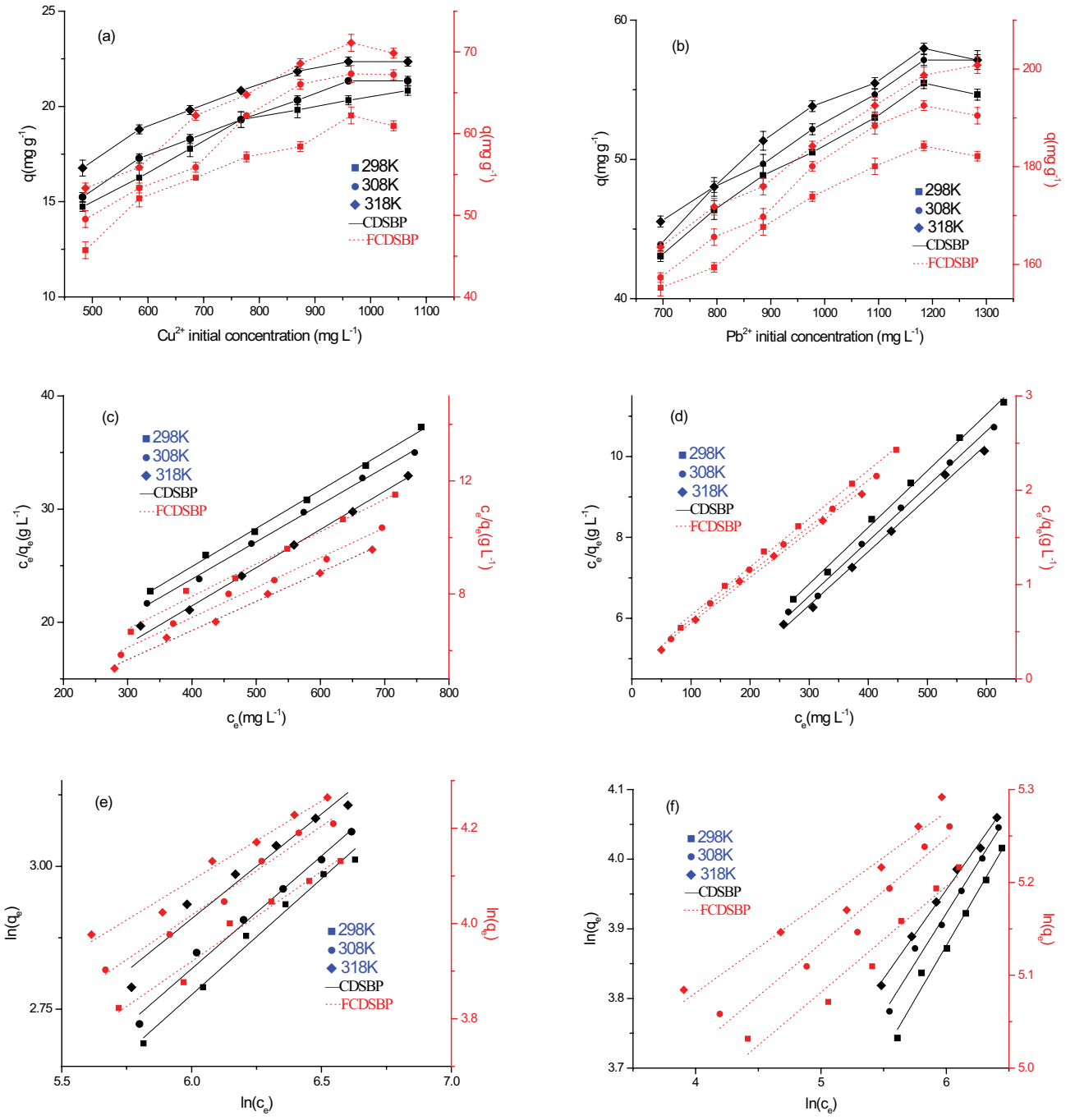


Fig. 6. Effect of the initial concentration of (a) $Cu^{2+}$ and (b) $Pb^{2+}$ on the adsorption capacity of CDSBP and FCDSBP: 0.5 CDSBP or 0.2 g of FCDSBP mixed with 50 mL $Ca^{2+}$ or $Pb^{2+}$ solution, respectively, at 50°C and pH = 4.5; Adsorption isotherms of (c) $Cu^{2+}$ and (d) $Pb^{2+}$ according to the Langmuir model; Adsorption isotherms of (e) $Cu^{2+}$ and (f) $Pb^{2+}$ according to the Freundlich model.

and 1,200 mg $L^{-1}$ for $Pb^{2+}$. However, the variation of adsorption capacity was negligible with the increasing in metal ion concentration. This result indicated a limitation of the adsorption process. This might be attributed to an increase in the driving force of the concentration gradient with the increase of initial metal ion concentration [50]. In addition, the adsorption capacity of CDSBP and FCDSBP for $Cu^{2+}$ and $Pb^{2+}$ increased with temperature.

Adsorption isotherms of $Cu^{2+}$ and $Pb^{2+}$ on CDSBP and FCDSBP are shown in Fig. 6. The relative adsorption parameters calculated from the Langmuir and Freundlich models were listed in Table 1. A high correlation coefficient ($R^2$) represented a good regression. The Langmuir isotherm model, with all of the correlation coefficients values were greater than 0.98, was a better fit than the Freundlich model for the adsorption data in the temperature range from 298 to 318 K,

Table 1
Parameters of the Langmuir and Freundlich isotherms

| Metals | Adsorbent | Temp (K) | Langmuir | | | Freundlich | | |
|---|---|---|---|---|---|---|---|---|
| | | | $q_m$ (mg g$^{-1}$) | $K_L$ (L mg$^{-1}$) | $R^2$ | $K_F$ | $1/n$ | $R^2$ |
| $Cu^{2+}$ | CDSBP | 298 K | 29.62 | 0.00295 | 0.9975 | 1.405 | 0.4058 | 0.9843 |
| | | 308 K | 30.41 | 0.00308 | 0.9972 | 1.571 | 0.3948 | 0.9857 |
| | | 318 K | 30.71 | 0.00374 | 0.9949 | 2.031 | 0.3665 | 0.9441 |
| | FCDSBP | 298 K | 87.25 | 0.00344 | 0.9897 | 5.214 | 0.3782 | 0.9692 |
| | | 308 K | 94.42 | 0.00361 | 0.9892 | 5.906 | 0.3734 | 0.9806 |
| | | 318 K | 97.08 | 0.00397 | 0.9954 | 8.103 | 0.3331 | 0.9738 |
| $Pb^{2+}$ | CDSBP | 298 K | 71.47 | 0.00527 | 0.9958 | 7.546 | 0.3091 | 0.9821 |
| | | 308 K | 73.52 | 0.00551 | 0.9951 | 9.043 | 0.2867 | 0.9826 |
| | | 318 K | 75.36 | 0.00567 | 0.9938 | 11.311 | 0.2549 | 0.9935 |
| | FCDSBP | 298 K | 195.31 | 0.0314 | 0.9973 | 90.017 | 0.1141 | 0.9491 |
| | | 308 K | 203.25 | 0.0357 | 0.9971 | 96.377 | 0.1132 | 0.9572 |
| | | 318 K | 205.76 | 0.0457 | 0.9962 | 109.001 | 0.0974 | 0.9381 |

indicating that the adsorption of metal ions ($Cu^{2+}$ and $Pb^{2+}$) onto CDSBP and FCDSBP was homogeneous monolayer coverage. Furthermore, the maximum adsorption capacity of CDSBP and FCDSBP for $Cu^{2+}$ and $Pb^{2+}$ was 30.71 and 97.08 mg g$^{-1}$, 75.36 and 205.76 mg g$^{-1}$, respectively. FCDSBP exhibited larger adsorption capacity for $Cu^{2+}$ and $Pb^{2+}$ ions than CDSBP.

Moreover, many researchers have investigated other natural biomass as low-cost biosorbents to remove metal ions. The adsorption performances of CDSBP and FCDSBP were also compared with other adsorbents (Table 2). However, it should be noted that the results presented in Table 2 were based on experiments conducted under different operating conditions. In general, sugar beet pulp was a superior adsorbent compared with other natural bio-adsorbent materials, and the maximum adsorption capacity of FCDSBP was higher than other reported adsorbents, indicating that this chemical modification of de-pectinated pulp was a great success. Additionally, the good adsorption performance of heavy metal and unsophisticated production process would provide great potential and broad prospects for FCDSBP wider application in wastewater treatment.

### 3.5. Adsorption kinetics

Fig. 7 shows that the equilibrium time was achieved after 5 and 15 min for $Cu^{2+}$; 15 and 20 min for $Pb^{2+}$ for CDSBP and FCDSBP, respectively. The uptake of $Cu^{2+}$ and $Pb^{2+}$ increased rapidly in the beginning and then increased slowly until the system reaches equilibrium.

Adsorption kinetics describes the uptake rate of the adsorbate and its residence time. The results first showed a rapid increase in adsorption capacity for each ion on CDSBP and FCDSBP, followed by a slow increase. Initially, the driving force was high due to the concentration difference between the solid–liquid interface and the solution,

Table 2
Reported adsorption capacities for several natural materials

| Adsorbent | $q_{max}$ (mg g$^{-1}$) | | Reference |
|---|---|---|---|
| | $Cu^{2+}$ | $Pb^{2+}$ | |
| Saw dust | 1.79 | 3.19 | [51] |
| Wheat bran | 14.50 | 63.90 | [52] |
| Activated carbon cloth | 15.30 | 17.20 | [53] |
| Leaves | – | 58.85 | [11] |
| Sunflower stalks | 29.30 | – | [54] |
| Sugar beet pulp pectin gels | 31.25 | 83.33 | [36] |
| Acid modified orange peel | 15.27 | 73.53 | [55] |
| Polymerized pine bark | 45.05 | 41.50 | [56] |
| Tartaric acid modified rice husk | 29.00 | 108.00 | [20] |
| EDTA dianhydride modified mercerized cellulose | 47.60 | 192.00 | [23] |
| CDSBP | 30.71 | 75.36 | This paper |
| FCDSBP | 97.08 | 205.76 | This paper |

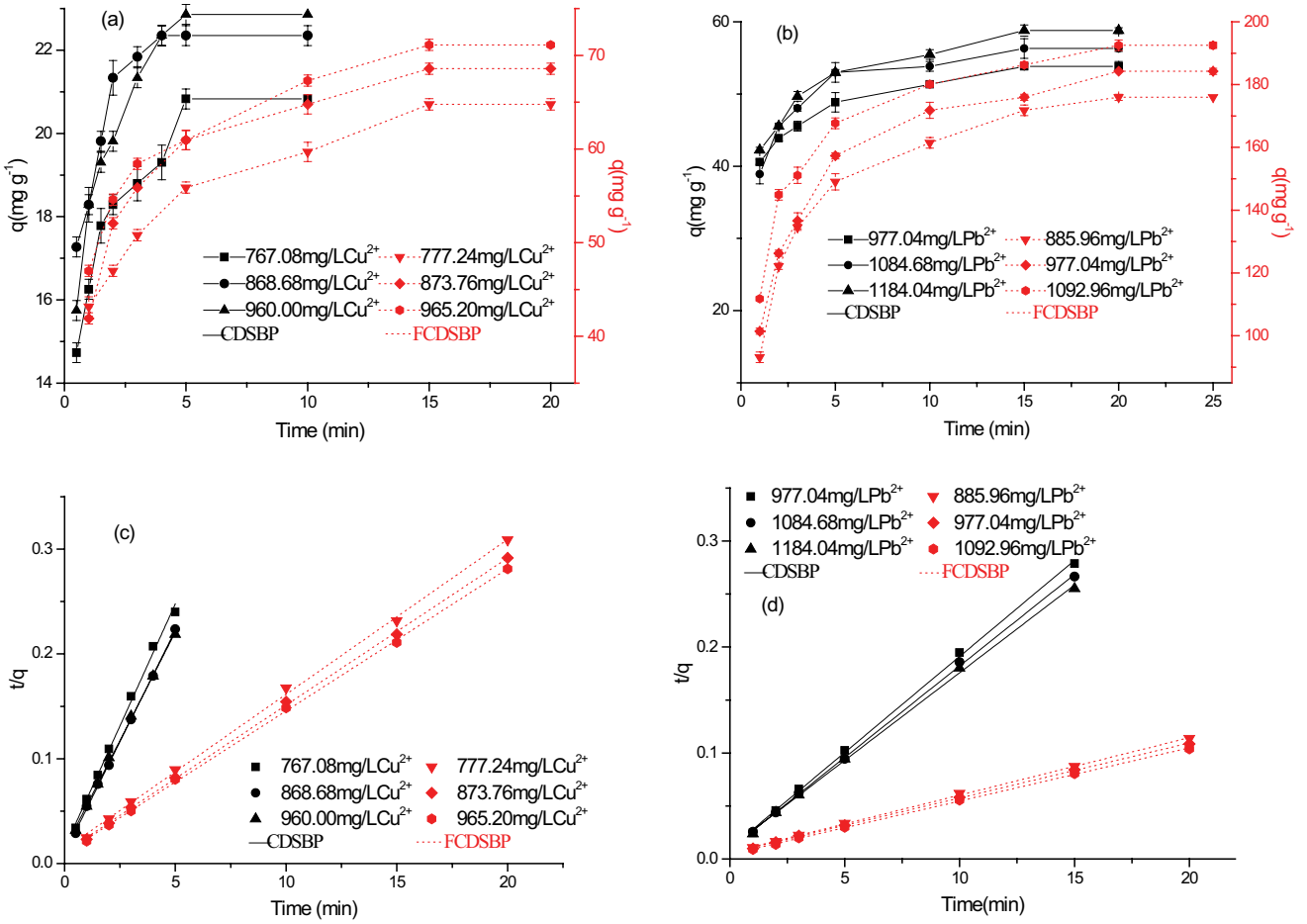


Fig. 7. Adsorption of (a) $Cu^{2+}$ and (b) $Pb^{2+}$ on CDSBP and FCDSBP over time: 0.5 CDSBP or 0.2 g of FCDSBP mixed with 50 mL $Ca^{2+}$ or $Pb^{2+}$ solution, respectively, at 50°C and pH = 4.5; Pseudo-second-order model for the removal of (c) $Cu^{2+}$ and (d) $Pb^{2+}$ by CDSBP and FCDSBP.

leading to a high adsorption rate [57]. In this study, the first-order model and the second-order model were fitted to experimental data and to describe the dynamic adsorption. The Lagergren pseudo-first-order model is illustrated in Eqs. (4) and (5):

$$\frac{d_q}{d_t} = K_1\left(q_e - q_t\right) \tag{4}$$

$$\ln\left(q_e - q_t\right) = \ln q_e - K_1 t \tag{5}$$

The pseudo-second-order model can be expressed in Eqs. (6) and (7) as follows:

$$\frac{d_q}{d_t} = K_2\left(q_e - q_t\right)^2 \tag{6}$$

$$\frac{t}{q_t} = \frac{1}{K_2 q_e^2} + \frac{t}{q_e} \tag{7}$$

In Eqs. (4)–(7), $q_t$ and $q_e$ are the amount of metal ions adsorbed per gram of adsorbent (mg $g^{-1}$) at any time $t$ and at the equilibrium time, respectively, and $K_1$ and $K_2$ are the adsorption rate constants.

The experimental data were fitted to the linear form of the two models, and the calculated kinetic parameters were summarized in Table 3. By comparing the squared correlation coefficient $R^2$ of the two kinetic models, it was found that the pseudo-second-order model provides better correlation than the pseudo-first-order model. Moreover, the plots of $t/q$ against $t$ for the linear second-order model are shown in Fig. 7. The $q_{pre}$ values obtained using pseudo-second-order equation were quite close to the experimental $q_{exp}$ values at different initial metal ion concentration. This further indicated that the adsorption of metal ions ($Cu^{2+}$ and $Pb^{2+}$) on CDSBP and FCDSBP follows the second-order kinetics.

### 3.6. Adsorption thermodynamics

To determine the thermodynamic properties of metal ions ($Cu^{2+}$ and $Pb^{2+}$), removal by CDSBP and FCDSBP, three basic thermodynamic parameters such as Gibbs free energy change ($\Delta G°$, kJ $mol^{-1}$), enthalpy change ($\Delta H°$, kJ $mol^{-1}$)

Table 3
Kinetic parameters for the adsorption of metal ions by CDSBP and FCDSBP at all studied concentration

| Metal | Adsorbent | Initial solution concentration (mg $L^{-1}$) | Lagergren first-order kinetic model | | | Experimental adsorption capacity $q_{exp}$ (mg $g^{-1}$) | Pseudo-second-order model | | |
|---|---|---|---|---|---|---|---|---|---|
| | | | $q_e$ (mg $g^{-1}$) | $k_1$ ($min^{-1}$) | $R^2$ | | Predicted adsorption capacity $q_{pre}$ (mg $g^{-1}$) | Rate constant $k_2$ (mg $g^{-1}$ $min^{-1}$) | $R^2$ |
| $Cu^{2+}$ | CDSBP | 767.08 | 6.33 | 0.3808 | 0.9196 | 20.83 | 21.45 | 0.1464 | 0.995 |
| | | 868.68 | 7.02 | 0.6641 | 0.9808 | 22.35 | 23.48 | 0.1837 | 0.999 |
| | | 960.00 | 10.07 | 0.7003 | 0.9564 | 22.86 | 24.16 | 0.1226 | 0.998 |
| | FCDSBP | 777.24 | 24.65 | 0.1675 | 0.9392 | 64.77 | 67.65 | 0.0153 | 0.998 |
| | | 873.76 | 25.33 | 0.2001 | 0.9367 | 68.58 | 71.27 | 0.0180 | 0.999 |
| | | 965.20 | 24.46 | 0.1923 | 0.9505 | 71.12 | 73.69 | 0.0186 | 0.999 |
| $Pb^{2+}$ | CDSBP | 977.04 | 14.43 | 0.1830 | 0.9712 | 53.82 | 55.18 | 0.0331 | 0.998 |
| | | 1,084.68 | 16.48 | 0.2064 | 0.8749 | 56.31 | 57.93 | 0.0313 | 0.999 |
| | | 1,184.04 | 17.33 | 0.1765 | 0.9247 | 58.79 | 60.45 | 0.0263 | 0.998 |
| | FCDSBP | 885.96 | 83.76 | 0.1959 | 0.974 | 175.95 | 184.50 | 0.0049 | 0.999 |
| | | 977.04 | 82.39 | 0.1803 | 0.973 | 184.23 | 192.68 | 0.0047 | 0.999 |
| | | 1,092.96 | 72.28 | 0.1707 | 0.958 | 192.51 | 199.21 | 0.0057 | 0.999 |

and entropy change ($\Delta S°$, J $mol^{-1}$ $K^{-1}$) were calculated by Eqs. (8)–(10):

$$K_D = \frac{q_t}{C_t} \tag{8}$$

$$\ln K_D = \frac{\Delta S°}{R} - \frac{\Delta H°}{RT} \tag{9}$$

$$\Delta G° = \Delta H° - \Delta S° \tag{10}$$

where $K_D$ (L $g^{-1}$) is the distribution coefficient, $R$ (8.314 J $mol^{-1}$ $K^{-1}$) is the universal gas constant and $T$ (K) is the adsorption temperature.

All the thermodynamic parameters were calculated and listed in Table 4. The negative values of $\Delta G°$ at all experimental temperatures indicated the sorption of metal ions ($Cu^{2+}$ and $Pb^{2+}$) on CDSBP and FCDSBP was spontaneous and thermodynamically feasible. In addition, the values of $\Delta G°$ became more negative from 298 to 318 K, indicating that spontaneity increased with increasing temperature. The enhancement of spontaneity could be favorable to the equilibrium adsorption capacity of metal ions, which can be observed in Fig. 6. The $\Delta H°$ value was positive, verifying that metal ions removal by CDSBP and FCDSBP was an endothermic adsorption process. The positive $\Delta S°$ value indicated that, when metal ions adsorption occured, the degree of freedom at the solid–liquid interface increased owing to the lower affinity of metal ions for the active adsorption sites of adsorbent than that of the exchange ions [58].

### 3.7. Adsorption mechanisms

Multiple studies have shown that complexation positively affects the accumulation removal mechanism of metal

Table 4
Thermodynamic parameters for metal ions adsorbed on CDSBP and FCDSBP

| Metals | Adsorbent | Temp (K) | $K_D$ (L $g^{-1}$) | $\Delta G°$ (kJ $mol^{-1}$) | $\Delta H°$ (kJ $mol^{-1}$) | $\Delta S°$ (J $mol^{-1}$ $K^{-1}$) |
|---|---|---|---|---|---|---|
| $Cu^{2+}$ | CDSBP | 298 K | 1.32 | –0.61 | 36.01 | 122.85 |
| | | 308 K | 1.91 | –1.83 | | |
| | | 318 K | 3.3 | –3.06 | | |
| | FCDSBP | 298 K | 1.27 | –0.68 | 35.27 | 120.63 |
| | | 308 K | 2.3 | –1.88 | | |
| | | 318 K | 3.1 | –3.09 | | |
| $Pb^{2+}$ | CDSBP | 298 K | 1.2 | –0.39 | 28.21 | 96.01 |
| | | 308 K | 1.62 | –1.36 | | |
| | | 318 K | 2.46 | –2.32 | | |
| | FCDSBP | 298 K | 1.85 | –1.49 | 22.16 | 79.37 |
| | | 308 K | 2.37 | –2.28 | | |
| | | 318 K | 3.25 | –3.08 | | |

ion [20,37]. And the metal speciation was a significant contribution to the adsorption in a given water system.

The functional groups on the surface of CDSBP such as –C=O, –OH, and –COOH have an important contribution to the adsorption of metal ions. However, perhaps the most significant contribution originates from citric acid grafted on CDSBP. The adsorption of $Cu^{2+}$ and $Pb^{2+}$ onto CDSBP composite might be based on the intermolecular forces such as electrostatic attraction, ion-exchange interaction and especially metal–ligand complexation [59]. Citric acid possesses three hydroxyl groups and three carboxyl groups that are available to chelate metal ions. The grafted CA would improve the adsorption capacity of the CDSBP by providing additional CA–metal chelation interactions between the modified sugar beet pulp and metal ions (Fig. 8a).

From the experimental data of adsorption on metal ions ($Cu^{2+}$ and $Pb^{2+}$) by CDSBP and FCDSBP, it could be observed that FCDSBP was capable of adsorbing significantly higher heavy metal concentrations than CDSBP. Owing to strongly basic conditions during the preparation of the FCDSBP, the surface carboxyl groups lost their hydrogen ions and became negatively charged, $Fe^{3+}$ ions could form various Fe species and occupied these negatively charged sites [60]. In addition, the presence of amorphous Fe species on FCDSBP was also confirmed by its XRD spectrogram, since neither a notable change in the basic cellulose diffraction peaks nor the presence of additional Fe oxides or oxo-hydroxidic crystalline phases was detected [61]. It was evident that amorphous Fe-oxide species on external surfaces of fiber positively affected the adsorption capacity of metal ions and had an more important contribution to the adsorption of $Cu^{2+}$ and $Pb^{2+}$ than complexation. Furthermore, the previous studies by other researchers have proposed that extra-framework metallic cations could be deposited on external surfaces of adsorbent and the active species may be the binuclear $[HO–Fe–O–Fe–OH]^{2+}$ clusters [62]. The IR analysis has shown the increase in hydrogen bonding. If not structurally hydroxylated, as shown in Fig. 8b, Fe atoms in an aqueous complex with water and form coordination shell of nearest neighbour [33]. Afterwards, the formed hydroxylated oxide

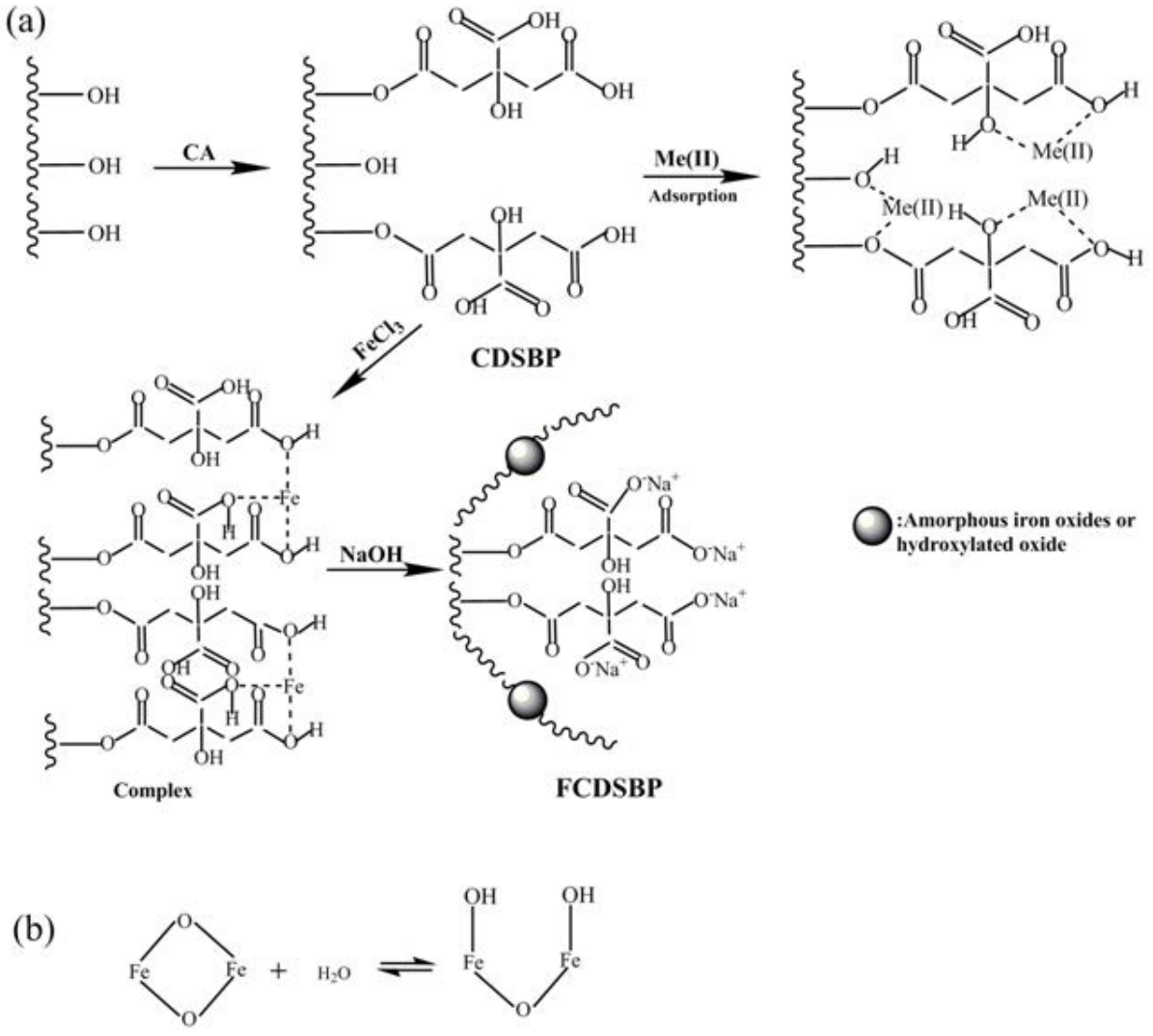


Fig. 8. Speculated adsorption mechanism (a) of metal ions and formation reaction (b) of hydroxylated oxide.

forms hydrogen bonds with other water molecules. In general, the metal ions ($Cu^{2+}$ and $Pb^{2+}$) adsorption capacity of FCDSBP increased significantly by amorphous iron oxides of $FeO_x$ type and hydroxylated oxide located at the surface of adsorbent.

## 4. Conclusion

The present investigation showed that FCDSBP was a potential biosorbent for the removal of heavy metal from an aqueous medium by loading of amorphous Fe-oxide species on external surfaces of fiber. Due to the presence of the amorphous Fe-oxide phase and hydroxylated oxide, FCDSBP was capable of adsorbing significantly higher $Cu^{2+}$ and $Pb^{2+}$ concentrations than CDSBP prepared by introducing citric acid to SBP fiber surface through an esterification reaction. In relation to CDSBP, FCDSBP presented an increase in adsorption capacity for $Cu^{2+}$ (66.37 mg $g^{-1}$) and $Pb^{2+}$ (130.4 mg $g^{-1}$). In addition, the Langmuir isotherm model and the pseudo-second-order model fitted well to the adsorption equilibrium data. The thermodynamic parameters suggested that the adsorption of metal ions ($Cu^{2+}$ and $Pb^{2+}$) by CDSBP and FCDSBP was endothermic and spontaneous in nature. Considering FCDSBP has not been extensively studied yet, further studies, such as the identification of the best preparation conditions, its complete characterization and the adsorption and desorption cycles for removing metal ions, should be carried out and given more considerable attention.

## Acknowledgments

The authors thank the financial support received from the National Natural Science Foundation of China (NSFC) foundation (U1203183), the Xinjiang Natural Science Foundation of China (2018D01A03), the Science and Technology Innovation team's construction Foundation in Xinjiang Uygur Autonomous Region (2014751002) and the Science and Technology Planning Project of the Xinjiang Production and Construction Corps, China (2018AB009).

## References

[1] B.K. Bansod, T. Kumar, R. Thakur, S. Rana, I. Singh, A review on various electrochemical techniques for heavy metal ions detection with different sensing platforms, Biosens. Bioelectron., 94 (2017) 443–455.
[2] J.-G. Yu, B.-Y. Yue, X.-W. Wu, Q. Liu, F.-P. Jiao, X.-Y. Jiang, X.-Q. Chen, Removal of mercury by adsorption: a review, Environ. Sci. Pollut. Res., 23 (2016) 5056–5076.
[3] Y. Chen, B. Pan, S. Zhang, H. Li, L. Lv, W. Zhang, Immobilization of polyethylenimine nanoclusters onto a cation exchange resin through self-crosslinking for selective Cu(II) removal, J. Hazard. Mater., 190 (2011) 1037–1044.
[4] B. Alyüz, S. Veli, Kinetics and equilibrium studies for the removal of nickel and zinc from aqueous solutions by ion exchange resins, J. Hazard. Mater., 167 (2009) 482–488.
[5] H. Cheng, Cu(II) Removal from lithium bromide refrigerant by chemical precipitation and electrocoagulation, Sep. Purif. Technol., 52 (2006) 191–195.
[6] J. Goel, K. Kadirvelu, C. Rajagopal, G.V. Kumar, Removal of lead(II) by adsorption using treated granular activated carbon: batch and column studies, J. Hazard. Mater., 125 (2005) 211–220.
[7] C.P. Dwivedi, J.N. Sahu, C.R. Mohanty, B.R. Mohan, B.C. Meikap, Column performance of granular activated carbon packed bed for Pb(II) removal, J. Hazard. Mater., 156 (2008) 596–603.
[8] F. Fu, Q. Wang, Removal of heavy metal ions from wastewaters: a review, J. Environ. Manage., 92 (2011) 407–418.
[9] A.G. El Samrani, B.S. Lartiges, F. Villiéras, Chemical coagulation of combined sewer overflow: heavy metal removal and treatment optimization, Water Res., 42 (2008) 951–960.
[10] S. Chen, Q. Yue, B. Gao, X. Xu, Equilibrium and kinetic adsorption study of the adsorptive removal of Cr(VI) using modified wheat residue, J. Colloid Interface Sci., 349 (2010) 256–264.
[11] F. Boudrahem, F. Aissani-Benissad, A. Soualah, Adsorption of lead(II) from aqueous solution by using leaves of date trees as an adsorbent, J. Chem. Eng. Data, 56 (2011) 1804–1812.
[12] D. Shukla, P.S. Vankar, Efficient biosorption of chromium(VI) ion by dry Araucaria leaves, Environ. Sci. Pollut. Res., 19 (2012) 2321–2328.
[13] S. Chakravarty, A. Mohanty, T.N. Sudha, A.K. Upadhyay, J. Konar, J.K. Sircar, A. Madhukar, K.K. Gupta, Removal of Pb(II) ions from aqueous solution by adsorption using bael leaves (*Aegle marmelos*), J. Hazard. Mater., 173 (2010) 502–509.
[14] C. Jeon, Removal of copper ion using rice hulls, J. Ind. Eng. Chem., 17 (2011) 517–520.
[15] M.M. Zulkali, A.L. Ahmad, N.H. Norulakmal, *Oryza sativa* L. husk as heavy metal adsorbent: optimization with lead as model solution, Bioresour. Technol., 97 (2006) 21–25.
[16] K. Huang, Y. Xiu, H. Zhu, Selective removal of Cr(VI) from aqueous solution by adsorption on mangosteen peel, Environ. Sci. Pollut. Res., 20 (2013) 5930–5938.
[17] S. Wan, Z. Ma, Y. Xue, M. Ma, S. Xu, L. Qian, Q. Zhang, Sorption of Lead(II), Cadmium(II), and Copper(II) Ions from aqueous solutions using tea waste, Ind. Eng. Chem. Res., 53 (2014) 3629–3635.
[18] R.S. Praveen, K. Vijayaraghavan, Optimization of Cu(II), Ni(II), Cd(II) and Pb(II) biosorption by red marine alga *Kappaphycus alvarezii*, Desal. Wat. Treat., 55 (2015) 1816–1824.
[19] W.S. Wan Ngah, M.A.K.M. Hanafiah, Removal of heavy metal ions from wastewater by chemically modified plant wastes as adsorbents: a review, Bioresour. Technol., 99 (2008) 3935–3948.
[20] K.K. Wong, C.K. Lee, K.S. Low, M.J. Haron, Removal of Cu and Pb by tartaric acid modified rice husk from aqueous solutions, Chemosphere, 50 (2003) 23–28.
[21] E.M. Soliman, S.A. Ahmed, A.A. Fadl, Removal of calcium ions from aqueous solutions by sugar cane bagasse modified with carboxylic acids using microwave-assisted solvent-free synthesis, Desalination, 278 (2011) 18–25.
[22] M. Jain, V.K. Garg, K. Kadirvelu, Removal of Ni(II) from aqueous system by chemically modified sunflower biomass, Desal. Wat. Treat., 52 (2014) 5681–5695.
[23] O.K. Júnior, L.V.A. Gurgel, R.P. de Freitas, L.F. Gil, Adsorption of Cu(II), Cd(II), and Pb(II) from aqueous single metal solutions by mercerized cellulose and mercerized sugarcane bagasse chemically modified with EDTA dianhydride (EDTAD), Carbohydr. Polym., 77 (2009) 643–650.
[24] C. Gérente, P.C. du Mesnil, Y. Andrès, J.-F. Thibault, P. Le Cloirec, Removal of metal ions from aqueous solution on low cost natural polysaccharides: sorption mechanism approach, React. Funct. Polym., 46 (2000) 135–144.
[25] E. Pehlivan, S. Cetin, B.H. Yanık, Equilibrium studies for the sorption of zinc and copper from aqueous solutions using sugar beet pulp and fly ash, J. Hazard. Mater., 135 (2006) 193–199.
[26] Z. Reddad, C. Gérente, Y. Andrès, M.-C. Ralet, J.-F. Thibault, P. Le Cloirec, Ni(II) and Cu(II) binding properties of native and modified sugar beet pulp, Carbohydr. Polym., 49 (2002) 23–31.
[27] Z. Aksu, I.A. Isoglu, Use of dried sugar beet pulp for binary biosorption of Gemazol Turquoise Blue-G reactive dye and copper(II) ions: equilibrium modeling, Chem. Eng. J., 127 (2007) 177–188.
[28] Z. Reddad, C. Gerente, Y. Andres, P. Le Cloirec, Mechanisms of Cr(III) and Cr(VI) removal from aqueous solutions by sugar beet pulp, Environ. Technol., 24 (2003) 257–264.

[29] N.M. El-Sawy, Z.I. Ali, Iron(III) complexed with radiation-grafted acrylic acid onto poly(tetrafluoroethylene-*co*-perfluorovinyl ether) films, J. Appl. Polym. Sci., 103 (2007) 4065–4071.
[30] T. Abe, M. Kaneko, Reduction catalysis by metal complexes confined in a polymer matrix, Prog. Polym. Sci., 28 (2003) 1441–1488.
[31] M. Du, C.-P. Liu, C.-S. Li, S.-M. Fang, Design and construction of coordination polymers with mixed-ligand synthetic strategy, Coord. Chem. Rev., 257 (2013) 1282–1305.
[32] W. Liu, J. Zhang, C. Zhang, Y. Wang, Y. Li, Adsorptive removal of Cr (VI) by Fe-modified activated carbon prepared from *Trapa natans* husk, Chem. Eng. J., 162 (2010) 677–684.
[33] M.K. Doula, Simultaneous removal of Cu, Mn and Zn from drinking water with the use of clinoptilolite and its Fe-modified form, Water Res., 43 (2009) 3659–3672.
[34] H. Fida, S. Guo, G. Zhang, Preparation and characterization of bifunctional Ti–Fe kaolinite composite for Cr(VI) removal, J. Colloid Interface Sci., 442 (2015) 30–38.
[35] E. Iakovleva, P. Maydannik, T.V. Ivanova, M. Sillanpää, W.Z. Tang, E. Mäkilä, J. Salonen, A. Gubal, A.A. Ganeev, K. Kamwilaisak, Modified and unmodified low-cost iron-coating solid wastes as adsorbents for efficient removal of As(III) and As(V) from mine water, J. Cleaner Prod., 133 (2016) 1095–1104.
[36] Y.N. Mata, M.L. Blázquez, A. Ballester, F. González, J.A. Muñoz, Sugar-beet pulp pectin gels as biosorbent for heavy metals: preparation and determination of biosorption and desorption characteristics, Chem. Eng. J., 150 (2009) 289–301.
[37] L.V.A. Gurgel, O. Júnior, R.P. de Freitas Gil, L.F. Gil, Adsorption of Cu(II), Cd(II), and Pb(II) from aqueous single metal solutions by cellulose and mercerized cellulose chemically modified with succinic anhydride, Carbohydr. Polym., 74 (2008) 922–929.
[38] J. Bolin, T. Peixin, Y. Kelu, S. Gang, Catalytic actions of alkaline salts in reactions between 1,2,3,4-butanetetracarboxylic acid and cellulose: II. Esterification, Carbohydr. Polym., 132 (2015) 228–236.
[39] B. Li, Y. Dong, L. Li, Preparation and catalytic performance of Fe(III)-citric acid-modified cotton fiber complex as a novel cellulose fiber-supported heterogeneous photo-Fenton catalyst, Cellulose, 22 (2015) 1295–1309.
[40] R.C. Sun, J. Tomkinson, Y.X. Wang, B. Xiao, Physico-chemical and structural characterization of hemicelluloses from wheat straw by alkaline peroxide extraction, Polymer, 41 (2000) 2647–2656.
[41] Y. Nishiyama, P. Langan, H. Chanzy, Crystal structure and hydrogen-bonding system in cellulose Iβ from synchrotron X-ray and neutron fiber diffraction, J. Am. Chem. Soc., 125 (2003) 14300–14306.
[42] D.V. Parikh, D.P. Thibodeaux, B. Condon, X-ray crystallinity of bleached and crosslinked cottons, Text. Res. J., 77 (2007) 612–616.
[43] B. Li, Y. Dong, M. Li, Z. Ding, Comparative study of different Fe(III)-carboxylic fiber complexes as novel heterogeneous Fenton catalysts for dye degradation, J. Mater. Sci., 49 (2014) 7639–7647.
[44] W. Xu, Effect of crosslinking treatment on the crystallinity, crystallite size, and strength of cotton fibers, Text. Res. J., 73 (2003) 433–436.
[45] P.N. Diagboya, E.D. Dikio, Scavenging of aqueous toxic organic and inorganic cations using novel facile magneto-carbon black-clay composite adsorbent, J. Cleaner Prod., 180 (2018) 71–80.
[46] R.P. Mohubedu, P.N.E. Diagboya, C.Y. Abasi, E.D. Dikio, F. Mtunzi, Magnetic valorization of biomass and biochar of a typical plant nuisance for toxic metals contaminated water treatment, J. Cleaner Prod., 209 (2019) 1016–1024.
[47] Z. Sun, Y. Liu, Y. Huang, X. Tan, G. Zeng, X. Hu, Z. Yang, Fast adsorption of $Cd^{2+}$ and $Pb^{2+}$ by EGTA dianhydride (EGTAD) modified ramie fiber, J. Colloid Interface Sci., 434 (2014) 152–158.
[48] E.I. Unuabonah, K.O. Adebowale, B.I. Olu-Owolabi, L.Z. Yang, L.X. Kong, Adsorption of Pb (II) and Cd (II) from aqueous solutions onto sodium tetraborate-modified Kaolinite clay: equilibrium and thermodynamic studies, Hydrometallurgy, 93 (2008) 1–9.
[49] P. Lodeiro, R. Herrero, M.E. Sastre de Vicente, The use of protonated *Sargassum muticum* as biosorbent for cadmium removal in a fixed-bed column, J. Hazard. Mater., 137 (2006) 244–253.
[50] Z. Aksu, Determination of the equilibrium, kinetic and thermodynamic parameters of the batch biosorption of nickel(II) ions onto *Chlorella vulgaris*, Process Biochem., 38 (2002) 89–99.
[51] A. Shukla, Y.-H. Zhang, P. Dubey, J.L. Margrave, S.S. Shukla, The role of sawdust in the removal of unwanted materials from water, J. Hazard. Mater., 95 (2002) 137–152.
[52] M.A. Farajzadeh, A.B. Monji, Adsorption characteristics of wheat bran towards heavy metal cations, Sep. Purif. Technol., 38 (2004) 197–207.
[53] K. Kadirvelu, C. Faur-Brasquet, P. Le Cloirec, Removal of Cu(II), Pb(II), and Ni(II) by adsorption onto activated carbon cloths, Langmuir, 16 (2000) 8404–8409.
[54] G. Sun, W. Shi, Sunflower stalks as adsorbents for the removal of metal ions from wastewater, Ind. Eng. Chem. Res., 37 (1998) 1324–1328.
[55] M.R. Lasheen, N.S. Ammar, H.S. Ibrahim, Adsorption/desorption of Cd(II), Cu(II) and Pb(II) using chemically modified orange peel: equilibrium and kinetic studies, Solid State Sci., 14 (2012) 202–210.
[56] M.E. Argun, S. Dursun, M. Karatas, Removal of Cd(II), Pb(II), Cu(II) and Ni(II) from water using modified pine bark, Desalination, 249 (2009) 519–527.
[57] X. Liu, L. Zhang, Removal of phosphate anions using the modified chitosan beads: adsorption kinetic, isotherm and mechanism studies, Powder Technol., 277 (2015) 112–119.
[58] Y. Khambhaty, K. Mody, S. Basha, B. Jha, Kinetics, equilibrium and thermodynamic studies on biosorption of hexavalent chromium by dead fungal biomass of marine *Aspergillus niger*, Chem. Eng. J., 145 (2009) 489–495.
[59] Z.-H. Wang, B.-Y. Yue, J. Teng, F.-P. Jiao, X.-Y. Jiang, J.-G. Yu, M. Zhong, X.-Q. Chen, Tartaric acid modified graphene oxide as a novel adsorbent for high-efficiently removal of Cu(II) and Pb(II) from aqueous solutions, J. Taiwan Inst. Chem. Eng., 66 (2016) 181–190.
[60] M. Doula, A. Ioannou, A. Dimirkou, Copper adsorption and Si, Al, Ca, Mg, and Na release from Clinoptilolite, J. Colloid Interface Sci., 245 (2002) 237–250.
[61] M.K. Doula, Synthesis of a clinoptilolite–Fe system with high Cu sorption capacity, Chemosphere, 67 (2007) 731–740.
[62] El.-M. El-Malki, R.A. van Santen, W.M.H. Sachtler, Introduction of Zn, Ga, and Fe into HZSM-5 cavities by sublimation: identification of acid sites, J. Phys. Chem. B, 103 (1999) 4611–4622.